J Mater Sci: Mater Med (2010) 21:3207–3215
DOI 10.1007/s10856-010-4164-8

Electrospinning of small diameter 3-D nanofibrous tubular scaffolds with controllable nanofiber orientations for vascular grafts

Huijun Wu · Jintu Fan · Chih-Chang Chu · Jun Wu

Received: 22 March 2010 / Accepted: 21 September 2010 / Published online: 2 October 2010

Abstract The control of nanofiber orientation in nanofibrous tubular scaffolds can benefit the cell responses along specific directions. For small diameter tubular scaffolds, however, it becomes difficult to engineer nanofiber orientation. This paper reports a novel electrospinning technique for the fabrication of 3-D nanofibrous tubular scaffolds with controllable nanofiber orientations. Synthetic absorbable poly-ε-caprolactone (PCL) was used as the model biomaterial to demonstrate this new electrospinning technique. Electrospun 3-D PCL nanofibrous tubular scaffolds of 4.5 mm in diameter with different nanofiber orientations (viz. circumferential, axial, and combinations of circumferential and axial directions) were successfully fabricated. The degree of nanofiber alignment in the electrospun 3-D tubular scaffolds was quantified by using the fast Fourier transform (FFT) analysis. The results indicated that excellent circumferential nanofiber alignment could be achieved in the 3-D nanofibrous PCL tubular scaffolds. The nanofibrous tubular scaffolds with oriented nanofibers had not only directional mechanical property but also could facilitate the orientation of the endothelial cell attachment on the fibers. Multiple layers of aligned nanofibers in different orientations can produce 3-D nanofibrous tubular scaffolds of different macroscopic properties.

H. Wu · J. Fan (✉)
Institute of Textiles and Clothing, The Hong Kong Polytechnic University, Hung Hom, Hong Kong
e-mail: tcfanjt@inet.polyu.edu.hk

C.-C. Chu
Department of Fiber Science and Apparel Design, Cornell University, Ithaca, NY 14853-4401, USA

J. Wu
Department of Biomedical Engineering, Cornell University, Ithaca, NY 14853, USA

1 Introduction

The search for ideal vascular substitute materials for cardiovascular applications as bypass or replacement of obstructed blood vessels due to diseases or trauma has far been a half-century endeavor [1, 2]. Polyethylene terephthalate (PET, Dacron) and expanded polytetrafluoroethylene (ePTFE) are the currently standard materials for large-diameter (>6 mm) vascular grafts [3], but no ideal alternative to autologous vein grafts is currently available for small-diameter (<5 mm) applications for its high failure rates owing to thrombosis, stenosis, and occlusion [4, 5]. Thus, finding a solution for small-diameter bypass grafting has recently become a major focus of attention. Integrating principles of tissue engineering with innovations of biomaterial technology is directed to develop new generations of vascular substitutes [2].

The extracellular matrix (ECM), composing of a basement membrane and a cross-linked network of proteins, glycosaminoglycans and collagen and elastin fibers with features in nanoscale, plays an important role in controlling cell behavior in living systems. In order to mimic the natural ECM, fabrication of nanofibers is one of the essential components for the development of an ideal scaffold for vascular grafts [6].

Electrospinning technique, which enables the production of continuous polymer micro- or nanofibers with diameters in the range of 50–5000 nm from polymer solutions or melts under high electric field, has been proposed as a promising alternative for fabricating vascular scaffolds because of its simplicity in setup, low cost productivity,

and facile control of fiber diameter and porosity [7–12]. Since the electrospun nanofibers have a high surface area to volume ratio, they provide more surface for cell attachment than other structures. With the electrospinning process, fibrous matrices in micro- or nano-scale dimensions have been fabricated from various natural polymers like collagen [13, 14] and fibrin [15] and a wide variety of absorbable synthetic polymers like poly-ε-caprolactone (PCL) [16, 17], poly(D-lactide) (PDLA) [18], poly(L-lactide) (PLLA) [19], and copolymers poly(L-lactide caprolactone) (P(LLA-CL) [20–23] and poly(D,L-lactide-co-glycolide) (PLGA) [24]. Tests on both in vitro and in vivo biocompatibility [4, 25–27] of these electrospun nanofibrous scaffolds confirmed the promise of using electrospun nanofiber scaffolds as vascular grafts substitutes, since they can effectively mimic the fine fibrous structure in connective and porous ECM [28–31].

Recently, it has been acknowledged that the two-dimensional (2-D) and three-dimensional (3-D) architecture of the electrospun nanofibers could regulate macroscopic mechanical properties and benefit cell differentiation, proliferation and functional longevity in tissue engineering scaffolds [32–34]. 2-D nanofiber membranes with uniaxially aligned arrays have been successfully fabricated by introducing insulating gaps into conductive collectors in the electrospinning process [35–38]. For specific applications in vascular grafts tissue engineering, 3-D nanofibrous tubular scaffolds with aligned nanofiber arrays are required to create cellular responses. It is known [32] that in the media layer of the native blood vessels, the SMCs and collagen fibrils have a marked circumferential orientation so as to provide the mechanical strength necessary to withstand the circulatory high pressures. The intima layer of the native blood vessels consists of a layer of endothelial cells lining the vessels internal surface. Between those two layers exists an internal elastic lamina mainly composed of elastin, which confers elastic properties to the blood vessels. Therefore, the ideal tubular scaffolds for vascular grafts may be the multilayered nanofibrous combination of an outer layer of circumferentially oriented nanofibers and an inner concentric layer of axial oriented nanofibers.

Rotating electro-conductive collectors of large diameter (e.g. rotating a disk collector with diameter of 20 cm [20], a cylindrical mandrel with a diameter of 4 cm [39] and an aluminum rod of 25.4 mm [40]) were used in electrospinning to produce 3-D nanofibrous tubes with fibre alignment. However, when small diameter rotating devices (e.g. rotating mandrel-type collectors with diameter of 6 mm [32]) was used, the fiber alignment was poor in the collected 3-D nanofibrous tubes. In order to improve fiber alignment in smaller diameter (<5 mm, 4.75 mm for example) vascular grafts scaffolds, Zhang and Chang [41] recently developed a technique based on manipulating the electric field through patterned protrusions. In their approach, aligned arrays were formed from the suspended nanofibers between protrusions, nevertheless disordered nanofiber arrays unavoidably occurred on the protrusions. Thus, there is a need to develop a more efficient and facile methods for the fabrication of small diameter 3-D nanofibrous tubes with controllable nanofiber orientations.

In this work, we demonstrate for the first time a novel electrospinning technique to fabricate the 3-D nanofibrous tubular scaffolds (especially small-diameter nanofibrous tubular scaffolds) with controllable nanofiber orientations through the combination of regulating the electric field and the rotation of the nanofiber collector. PCL was chosen as a model polymer for its lack of toxicity, low cost and degradability, and moreover, its well acknowledged role as model biomaterial for growing various cells [16, 17]. By using this novel technique, small diameter 3-D nanofibrous tubular scaffolds of different nanofiber orientations (e.g. circumferential orientation, axial orientation, and combined circumferential and axial orientations) were fabricated. Light microscopy and scanning emission microscopy (SEM) was used to capture images of electrospun scaffolds and fast Fourier transform (FFT) [33] was used to evaluate fiber alignment. DMA tests confirmed that the nanofibrous tubular scaffolds with oriented nanofibers had directional mechanical properties, and bovine endothelial cell culture data showed that fibre alignment in the electrospun nanofibrous material facilitated the orientation of the endothelial cell attachment on the fibers.

2 Materials and methods

2.1 Materials

Poly-ε-caprolactone (PCL, Mw 80,000, Sigma–Aldrich, St. Louis, MO) of 2 g was dissolved in 20 g chloroform (Sigma–Aldrich) under gentle magnetic stirring for several hours to obtain a homogeneous and stable solution. Then, 2 g DMF (Sigma–Aldrich) was added to the as-prepared PCL-chloroform solution to adjust the evaporation rate and solution surface tension of the polymer solution for electrospinning.

2.2 Electrospinning

Figure 1a and b illustrates the novel electrospinning technique used in our experiments to fabricate 3-D nanofibrous tubular scaffolds with circumferential (Fig. 1c) and axial (Fig. 1d) nanofiber orientations, respectively. Two metallic plates were separately placed with a distance of several centimeters apart and both connected to a DC negative

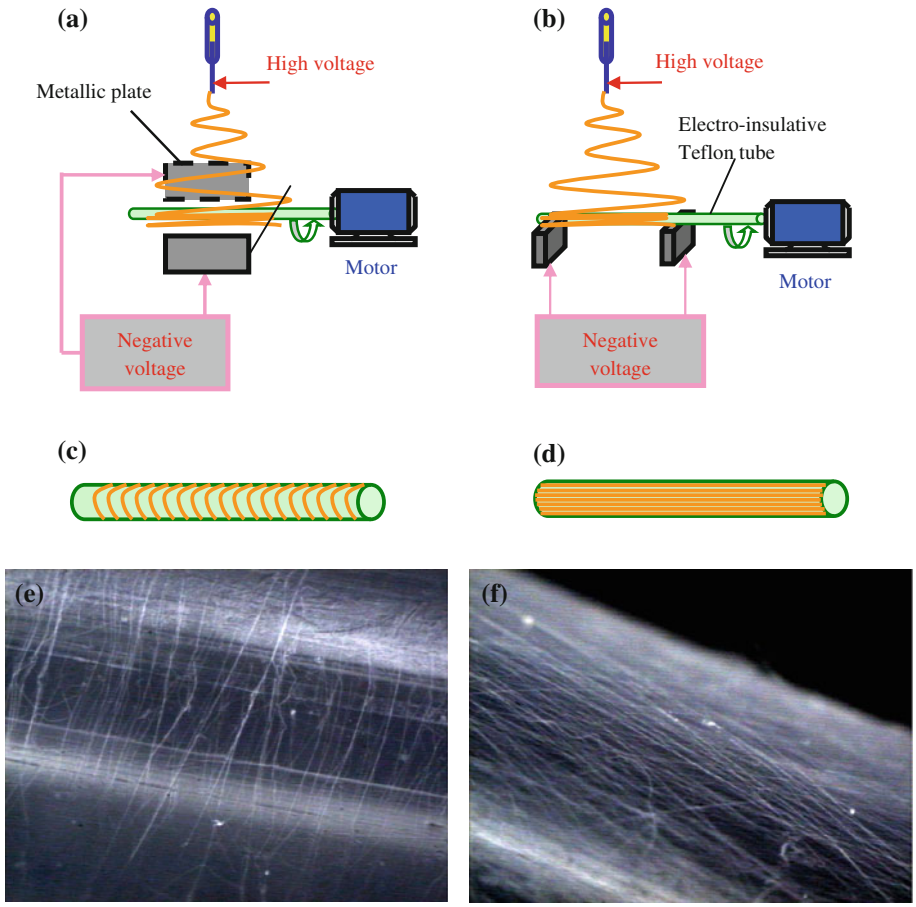

Fig. 1 Schematic illustration of electrospinning setup for fabrication of 3-D nanofibrous tubular scaffold with circumferential **a** and axial **b** nanofiber orientations. **c** and **d** illustrate the circumferential and axial nanofiber orientations, respectively. **e** and **f** are camera images of circumferentially and axially oriented nanofibers, respectively

voltage power supply (EMCO High Voltage Cooperation, Sutter Creek, CA) as the high voltage (EMCO High Voltage Cooperation) is applied to PCL solution for electrospinning. An electro-insulator Teflon rod connected to a rotating motor was introduced between the metallic plates as the collectors of the electrospun nanofibers. The rotation speed of the motor was suitably set at 300 rpm when collecting nanofibers in circumferential orientation, and at 50 rpm when collecting nanofibers in axial orientation.

For the process of electrospinning, the PCL solution was placed in a 10 ml plastic syringe fitted with a metal needle with tip diameter of 0.8 mm. Electrospun PCL nanofibers were electrospun at 18 kV as the high voltage and −2 kV as the negative voltage. The nanofiber collector was located 15 cm away from the charged metal needle tip. The feeding rate of the solution in the syringe was controlled at 0.4 ml/h by using a syringe pump.

In our experiments, the fabrication of the 3-D nanofibrous tubular scaffold was achieved through three steps. Firstly, aligned PCL nanofibers were electrospun by regulating the electric fields through the two separately placed metallic plates. Secondly, the aligned electrospun PCL nanofibers were collected by using the rotating electro-insulative Teflon rod. Thirdly, the electrospun 3-D nanofibrous tubular scaffolds with specific nanofibers orientation were obtained after the removal from the Teflon tube.

2.3 Light microscope

The morphology of the electrospun nanofibrous tubes was observed by using a camera (Model Nikon E3200) and an optical microscope (Model Nikon Optiphot).

2.4 Filed emission SEM

The morphology of electrospun nanofibers was investigated by using a SEM (JEOL JEM-6335F) at an accelerating voltage of 3–5 kV after coating the nanofibers with gold.

2.5 Fast fourier transform (FFT)

The FFT analysis was used to quantifiably evaluate the nanofiber alignment based on the SEM images of the as-electrospun 3-D PCL nanofibrous tubular scaffold. The FFT function converts information presented in an original data image (i.e. 'real space') into mathematically defined 'frequency space' [33, 42]. The resulting FFT output image

contains grayscale pixels that are distributed in a pattern that reflects the degree of the nanofiber alignment presented in the original data image.

A graphical plot of the FFT frequency distribution was generated by placing a circumferential projection on the FFT output image and conducting a circumferential summation of the pixel intensities for each degree between 0 and 360°, in 1° increments. It should be noted that the FFT data has been rotated 90° to correct for the mathematical transformation inherent to this type of analysis, allowing the principal axis of orientation to be directly determined from the position of the peak in the intensity plot. The extent of alignment presented in the original data image is reflected by the height and overall shape of the peak in the graphical plot of the FFT frequency distribution.

For our analysis, digitized SEM images were converted to 8-bit grayscale TIF files and cropped to 960 × 960 pixels. Images were processed with Image J software (NIH, http://rsb.info.nih.gov/ij) supported by an oval profile plug-in (authored by Bill O'Connell). All FFT data were normalized to a baseline value of 0 and plotted in arbitrary units, allowing different data sets to be directly compared.

2.6 DMA tests

A Perkin Elmer Diamond Dynamic Mechanical Analyzer (DMA) Lay System with a maximum strength length of 5 mm was used to determine the tensile properties (load-extension curves) of electrospun PCL scaffolds with aligned and random nanofiber orientations at an ambient temperature at a speed of 0.25 mm/min. Before the DMA tests, the electrospun PCL nanofibrous tubes were first cut open along the length direction into rectangular specimens of a typical size of 5 mm (length wise) × 10 mm (width wise).

2.7 Thickness measurements

The thicknesses of the specimens were determined using a Mitutoyo Litematic VL-50A.

2.8 Cell attachment on PCL electrospun nanofibrous membranes

The evaluation of the BAEC cell attachment on the PCL electrospinning fibrous membranes was performed by a live-cell assay, i.e. Calcein-AM assay (Invitrogen). Calcein-AM is a fluorescent probe precursor that enters into live cells and is then cleaved by intracellular esterases to form calcein, a cytosolic fluorescent marker. The non-oriented and oriented PCL fibrous membranes were cut into small pieces (1.5 cm × 1.5 cm) and sterilized under UV irradiation for 45 min in a cell culture hood, and placed carefully onto the 6 well cell culture plate, 70% ethanol sterilized metal rings with proper size were used to hold down the fibrous membranes. The Same amounts of BAEC cells at an appropriate cell density concentration (50,000 cells/well) were seeded onto each test well and then incubated in a 5% CO2 incubator at 37°C. Cell media was carefully changed every 2 days. After 4 days incubation, the cell culture plates were removed from the incubator, and the Calcein-AM assay was applied exactly following the manufacturer's protocol. Both the black-white and fluorescent images of cells and fibrous membranes were captured with a Zeiss Axio Observer.Z1 m with a Hamamatsu ORCA-ER camera. Images were pseudocolored with Axiovision software v. 4.6.

3 Results

3.1 Electrospun 3-D nanofibrous tubular scaffolds with axial and circumferential orientations

The camera images of the electrospun 3-D PCL nanofibers collected on the Teflon rod with diameter of 4.5 mm through the electrospinning technique are shown in Fig. 1e and f, respectively. The images show that the majority of the PCL nanofibers electrospun by the new fabrication technique depicted in Fig. 1a have the orientation along the circumferential direction of the Teflon rod. As a comparison, the majority of the PCL nanofibers electrospun through the technique depicted in Fig. 1b have the orientation along the axial direction of the Teflon rod. Therefore, depending on the relative positions and angular alignments of the metallic plates and the Teflon rod, the orientations of the electrospun PCL nanofiber collected on the Teflon rod can be readily regulated with the newly developed electrospinning technique.

Figure 2a shows the optical image of the 3-D PCL nanofibrous tubular scaffolds collected on Teflon rods of different size (diameters 3.2 mm, 4.5 mm and 7.6 mm). The electrospun 3-D PCL nanofibrous tubular scaffolds could be readily obtained by removing the Teflon rods. Figure 2b shows the optical images of an example PCL nanofibrous tubular scaffold of 4.5 mm diameter. Figure 2c and d shows the SEM images of the PCL nanofibrous scaffold in the frontal and cross-sectional views. The diameter of the PCL nanofibers was about 300–500 nm. Excellent alignment of electrospun PCL nanofibers along the circumferential direction was achieved as shown in Fig. 2c and d. From Fig. 2d the wall thickness of the electrospun PCL nanofibrous tubular scaffold were determined to be about 0.4 mm.

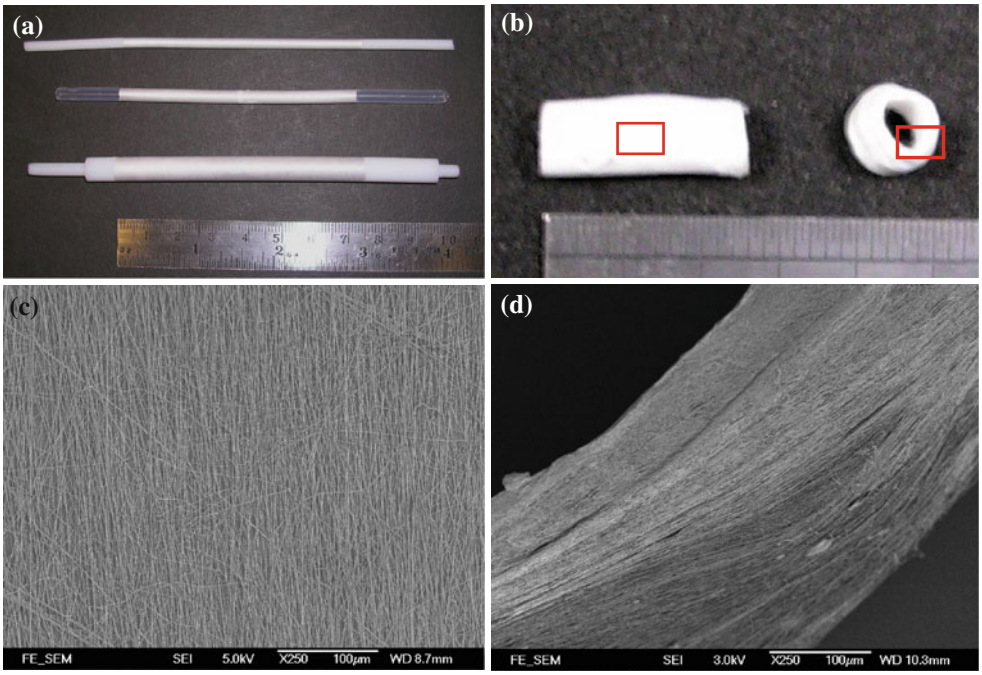

Fig. 2 Surface images of the electrospun 3-D nanofibrous tubular scaffold. **a** Camera images of the electrospun 3-D nanofibrous tubular scaffolds collected on Teflon tubes with different diameters: 3.2 mm (*top*), 4.5 mm (*middle*) and 7.6 mm (*bottom*): **b** Camera images of the electrospun 3-D nanofibrous tubular scaffolds after the removal of the Teflon tube with diameter of 4.5 mm: front view (*left*) and cross-section view (*right*). **c** and **d** are SEM images through the magnification of the patterns in **b**

3.2 Nanofiber alignment analysis of electrospun 3-D nanofibrous tubular scaffolds with axial and circumferential orientations

The FFT analysis of the SEM images [33] was also used to quantitatively analyze the degree of the PCL nanofiber alignment. In the FFT analysis, a graphical plot of the FFT frequency distribution was generated by summing the pixel intensities encountered along the radius of the FFT output image obtained from the original SEM image. Figure 3a shows the SEM images of the PCL nanofibrous tubular scaffold of diameter 4.5 mm, with nanofibres aligned in the circumferential direction. Figure 3b shows the FFT frequency distribution for the SEM image (at 500×) shown in Fig. 3a. A sharp peak with a normalized intensity of 0.26 can be observed at about 90.1°, confirming that most circumferentially oriented nanofibers were perpendicular (90° angle) to the axial direction of the tubular scaffold.

Figure 3c shows the SEM image for the electrospun 3-D PCL nanofibrous tubular scaffold of the diameter 4.5 mm with the axially oriented nanofibers. As can be seen, although the orientation was not as uniform as that for the circumferentially oriented nanofibers, majority of the nanofibers aligned along the axial direction of the tubular scaffold as also confirmed from the FFT frequency distribution shown in Fig. 3d, which indicates that the greatest intensity is located at the direction close to 0° against the axial direction of the tubular scaffold.

3.3 Multilayered nanofibrous tubular scaffolds with combined axial and circumferential orientations

By combining the circumferential and axial nanofiber electrospinning techniques as illustrated in Fig. 1a, b, electrospun 3-D multilayered PCL nanofibrous tubular scaffolds with combined axial and circumferential nanofiber orientations could be fabricated. Figure 4 shows the optical and SEM images of the 4.5 mm diameter electrospun 3-D multilayered PCL nanofibrous tubular scaffolds containing two nanofiber orientations. The inner most layer of PCL nanofibers were aligned along the axial direction of the tubular scaffold. Then, the circumferentially-oriented PCL nanofibers were deposited onto the first layer. It can be observed that most nanofibers of the bottom layer align along the axial direction of the tubular scaffold, while most nanofibers of the top layer align along the circumferential direction.

3.4 Tensile properties of nanofibrous tubular scaffolds with different nanofiber orientations

It is expected that different fiber orientation on the tubular scaffolds will result in different mechanical properties. Figure 5 plots the load-extension curves of the nanofibrous tubular scaffolds with axially, circumferentially and randomly oriented nanofibers, respectively, when the samples

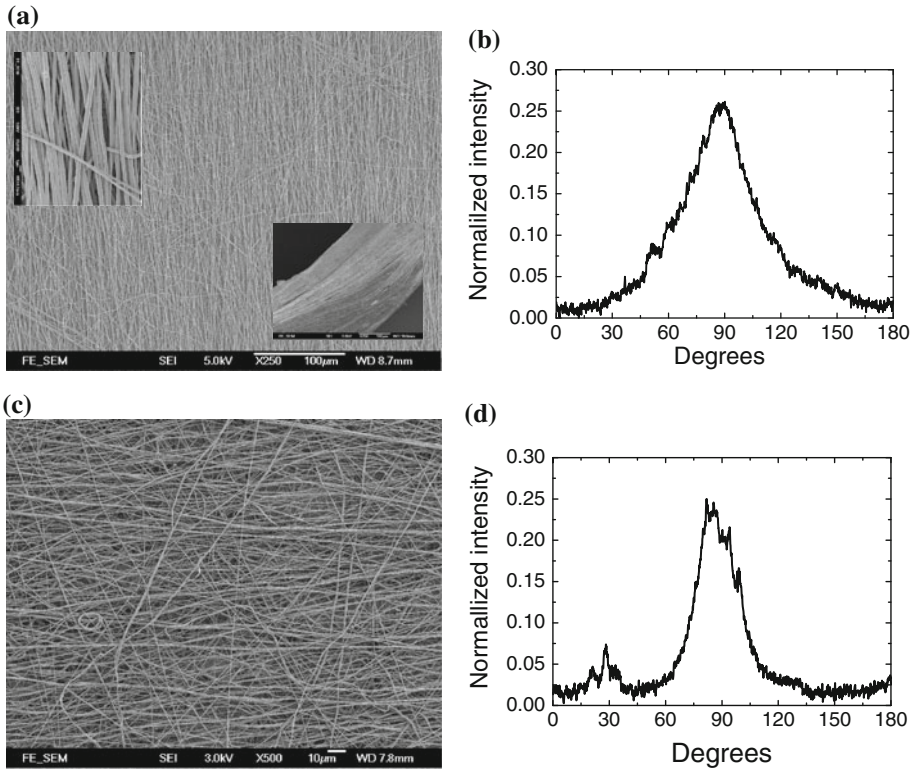

Fig. 3 **a** Surface SEM images of tubular scaffold with circumferentially oriented nanofibers; *top inset*: magnified image; *bottom inset*: cross-section view. **b** FFT analysis of tubular scaffold with circumferentially oriented nanofibers. **c** Surface SEM image and **d** FFT analysis of tubular scaffold with axial nanofiber orientation

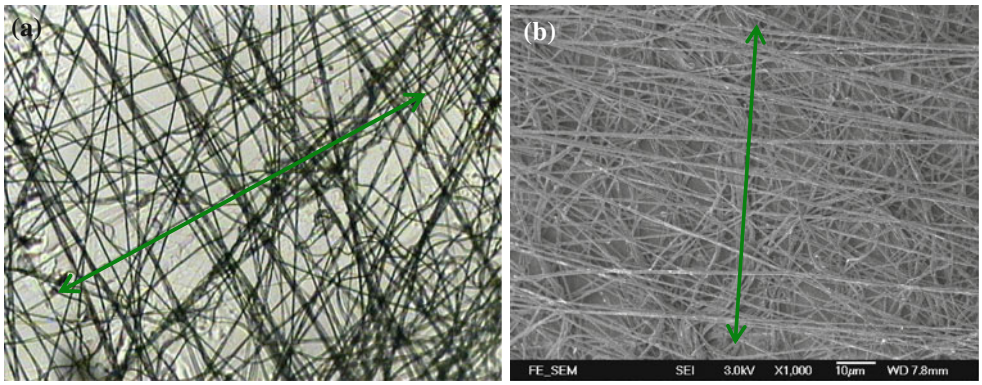

Fig. 4 Optical microscope (**a**) and SEM (**b**) images of the electrospun 3-D PCL nanofibrous tubular scaffold with combined axial and circumferential nanofiber orientations. The *arrow* indicate the axial direction of the Teflon tube

were stretched longitudinally along the axial direction on a DMA Lay System. As shown in Fig. 5, the load-extension curve of the tubular scaffold with axially oriented nanofibers was very different from the rest in that it had a significantly higher modulus (i.e. less extension at the same load) after the extension exceeded 20% and a relatively lower modulus when the extension was less than 20%. The low modulus at initial extension may be due to the straightening out of the sample during the initial period of the test, and the high modulus, when the extension exceeded 20%, was most probably caused by the extension of the nanofibres along their length direction. This finding is consistent with those of Li et al. [40] who also observed the increased Young's modulus of fiber-aligned scaffold, although the magnitude is different as it depends on many

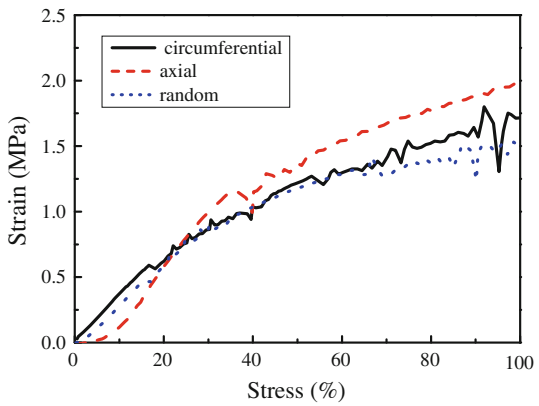

Fig. 5 Strain–stress curve of electrospun PCL nanofibrous tubular scaffolds pulled along the axial direction

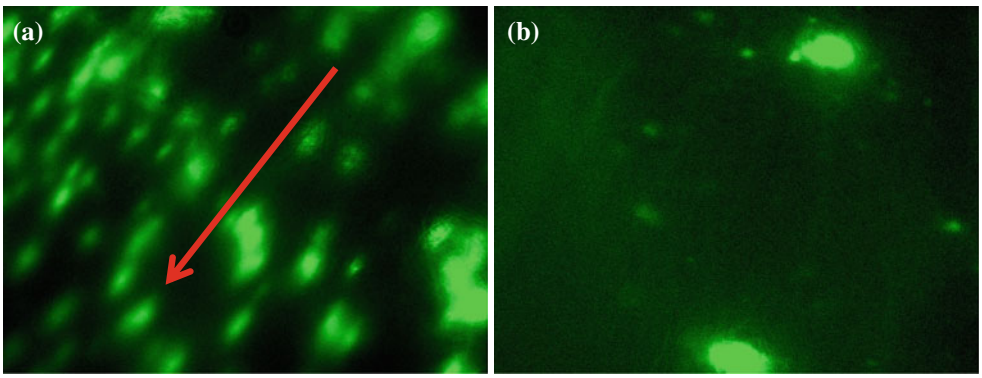

Fig. 6 Green-stained (in light shade) Calcein-AM assay of BAEC cells on aligned (**a**) and random (**b**) PCL electrospun fibrous membranes after 96 h incubation, 10×. The *arrow* indicates the direction of the oriented PCL fibers

processing parameters. The load-extension curve of the tubular scaffold with circumferentially oriented nanofibers was not too much different from that of the tubular scaffold with randomly oriented nanofibers. This is due to the fact that the circumferentially oriented nanofibers were not load-bearing as the specimens were stretched along the axial direction of the rod during the tests.

3.5 Cell response of nanofibrous tubular scaffolds with different nanofiber orientations

Figure 6 shows the Green-stained (in light shade) Calcein-AM assay of BAEC cells attached on the PCL aligned (Fig. 6a) and randomly (Fig. 6b) oriented electrospun fibrous membranes after 96 h incubation. As can be seen, the green-stained BAEC cells on the oriented PCL nanofibrous membrane (Fig. 6a) showed an elongated morphology and oriented along the same direction as the PCL electrospun fibrous membranes (arrow in the figure). On the contrary, the BAEC cells on the randomly PCL electrospun fibrous membrane (Fig. 6b) didn't show such elongated and oriented cell morphology along the direction of the PCL fibers. Therefore, both oriented and randomly-oriented PCL electrospun nanofibrous membranes support BAEC attachment and growth, but the oriented electrospinning fibrous membranes can facilitate and regulate the orientation of the endothelial cell attachment on the fibers. This finding is consistent to those reported by Li et al. [40], who found that hMSCs seeded on increasingly aligned scaffolds showed increased cellular alignment and formation of large stress fiber bundles.

4 Discussion

Fibre alignments in vascular grafts are essential for achieving mechanical compliance of blood vessels. One of the most frequent failure mode of synthetic vascular grafts is due to the mismatch in compliance between the synthetic vascular grafts and adjacent natural blood vessels. This mismatch in compliance is the most pronounced at the anastomotic site. Such a mismatch in compliance is mainly due to the mismatch in fibre orientation between the synthetic vascular grafts and adjacent natural blood vessels in addition to the mismatch in mechanical property of the synthetic fibers from the natural collagen and elastin fibers. In natural blood vessels, there are preferential collagen and elastin fibre orientations in the outermost layer (adventitia) of a blood vessel which provide successfully concentrical dilation and contraction during the diastolic and systolic cycles.

The availability of advanced electrospinning technology to fabricate tubular textile products has opened a new and viable option toward the design of fibrous-based synthetic vascular grafts that traditional textile fabrication methods can't achieve. Although 3-D nanofibrous tubular scaffolds of a diameter greater than 25 mm with good fibre alignments have been fabricated by rotating electro-conductive collectors during electrospinning [20, 39, 40], the fabrication of small diameter nanofibrous tubular scaffolds with good fibre alignment remains quite challenging [32]. For example, Zhang and Chang [41] attempted to improve fiber alignment in relatively small diameter (<5 mm) scaffolds through manipulating the electric field by patterned protrusions, but disordered nanofiber arrays unavoidably occurred on the protrusions.

In our current study reported in this paper, it is the first time that small diameter (<5 mm) nanofibrous tubular scaffolds with excellent fibre alignment could be fabricated using a special novel electrospinning technique. The orientations of the electrospun nanofibers depend on the relative positions and angular alignments of the metallic plates and the Teflon rod, and, therefore, the fibre orientation can be readily regulated with the newly developed electrospinning technique. The thickness of the nanofibrous

tubular scaffold can also be readily varied by regulating the electrospinning process parameters, especially the duration of the electrospinning process.

For the purpose of understanding how fibres are aligned during the electrospinning process, the electric field between the metallic plates and between the needle and the plates were analyzed by using the Student's QuickField program [36]. The electric field lines in the vicinity of the collector were split into two fractions pointing toward opposite edges of the gap. With the action of the electric field, the charged nanofibers experiences two sets of electric forces: one set originating from the splitting electric field and the other one between the positive charges on the nanofibers and the negative charges on the negative electrodes. Considering the Coulomb force are inversely proportional to the square of the separation between charges, the two ends of the fiber close to the metal electrodes generates stronger Coulomb force, which stretched the nanofibers across the gap and induced oriented nanofibers array between the two metallic plates. The aligned electrospun nanofibers array regulated the electric field were then collected by using the rotating electro-insulative Teflon rods to form 3-D tubular scaffolds. The rotating Teflon rod was introduced with its axial direction perpendicular to the direction of the aligned electrospun nanofiber array to form the 3-D nanofibrous tubular scaffold with circumferential nanofiber orientation. Similarly, the 3-D nanofibrous tubular scaffold with axial nanofibers orientation could be fabricated by introducing the Teflon rod with its axial direction along the aligned electrospun nanofibers array between the two metallic plates. It appears that the speed of the rotation of the Teflon rod does not impact the uniformity of collecting electrospun nanofibers. Moreover, the tangential force originating the rotation of the Teflon rod readily rolled the nanofibers on the Teflon rod.

In the present work, small diameter (i.e. 4.5 mm) electrospun nanofibrous tubular scaffolds containing two nanofiber orientations were produced with the newly developed electrospinning technique. It is believed that 3-D multilayered nanofibrous tubular scaffolds with complex nanofiber orientation architectures can also be readily fabricated by appropriately combining the two electrospinning techniques as illustrated in Fig. 1a, b.

As shown in Figs. 5 and 6, macroscopic mechanical property and cell responses are different with different nanofiber orientations. The nanofibrous tubular scaffolds with controllable nanofiber orientations as fabricated using the advanced electrospinning technique demonstrated in the present study is therefore advantageous in regulating the macroscopic mechanical property of the tubular scaffolds and benefit cell responses along different directions so as to better mimic the natural structure and biological responses of blood vessels.

5 Conclusions

A novel electrospinning technique was demonstrated to fabricate small diameter 3-D nanofibrous tubular scaffold with controllable nanofiber orientations so as to regulate the macroscopic mechanical property of the scaffolds and benefit cell responses along different directions for vascular grafts applications. The electrospun 3-D PCL nanofibrous tubular scaffold of diameter 4.5 mm with excellent nanofiber alignment along the circumferential direction and good alignment in the axial direction was successfully fabricated, respectively. The degree of nanofiber alignment was quantitatively evaluated by using the FFT analysis. By appropriately combining the two orientations of nanofibers in the multilayered nanofibrous tubular scaffolds, complex nanofiber orientation architectures can be readily constructed to achieve desirable macroscopic mechanical property and cell responses along specific directions for vascular graft applications. The nanofibrous tubular scaffolds with oriented nanofibers had directional mechanical property and could facilitate the orientation of the endothelial cell attachment on the fibers.

Acknowledgments Professor JT Fan and Dr HJ Wu would like to acknowledge the funding support of the Hong Kong Polytechnic University in the form of a Niche Area Project (1-BB82). This project is also partially supported by the Morgan seed grant program of Cornell University awarded to Professor CC Chu for the tissue engineering of vascular tissues.

References

1. Hass F. History of (micro) vascular surgery and the development of small-caliber blood vessel prostheses (with some notes on patency rates and re-endothelialization). Microsurgery. 1985;6:59–69.
2. Xue L, Greisler HP. Biomaterials in the development and future of vascular grafts. J Vasc Surg. 2003;37(2):472–80.
3. Gumpenberger T, Heitz J, Bauerle D, Kahr H, Graz I, Romanin C, et al. Adhesion and proliferation of human endothelial cells on photochemically modified polytetrafluoroethylene. Biomaterials. 2003;24(28):5139–44.
4. Lee SJ, Yoo JJ, Lim GJ, Atala A, Stitze J. In vitro evaluation of electrospun nanofiber scaffolds for vascular graft application. J Biomed Mater Res A. 2007;83A(4):999–1008.
5. Sayers RD, Raptis S, Berce M, Miller JH. Long-term results of femorotibial bypass with vein or polytetrafluoroethylene. Br J Surg. 1998;85(7):934–8.
6. Telemeco TA, Ayres C, Bowlin GL, Wnek GE, Boland ED, Cohen N, et al. Regulation of cellular infiltration into tissue engineering scaffolds composed of submicron diameter fibrils produced by electrospinning. Acta Biomater. 2005;1(4):377–85.
7. Fridrikh SV, Yu JH, Brenner MP, Rutledge GC. Controlling the fiber diameter during electrospinning. Phys Rev Lett. 2003;90(14):144502/144501–144504.
8. Greiner A, Wendorff JH. Electrospinning: a fascinating method for the preparation of ultrathin fibres. Angew Chem Int Ed. 2007;46(30):5670–703.

9. Li D, Xia YN. Electrospinning of nanofibers: reinventing the wheel? Adv Mater. 2004;16(14):1151–70.
10. Teo WE, Ramakrishna S. A review on electrospinning design and nanofibre assemblies. Nanotechnology. 2006;17(14):R89–106.
11. Wu HJ, Fan JT, Qin XH, Mo S, Hinestroza JP. Fabrication and characterization of a novel polypropylene/poly(vinyl alcohol)/aluminum hybrid layered assembly for high-performance fibrous insulation. J Appl Polym Sci. 2008;110(4):2525–30.
12. Wu HJ, Fan JT, Qin XH, Zhang GG. Thermal radiative properties of electrospun superfine fibrous PVA films. Mater Lett. 2008;62:828–31.
13. Rho KS, Jeong L, Lee G, Seo BM, Park YJ, Hong SD, et al. Electrospinning of collagen nanofibers: effects on the behavior of normal human keratinocytes and early-stage wound healing. Biomaterials. 2006;27(8):1452–61.
14. Buttafoco L, Kolkman NG, Engbers-Buijtenhuijs P, Poot AA, Dijkstra PJ, Vermes I, et al. Electrospinning of collagen and elastin for tissue engineering applications. Biomaterials. 2006;27(5):724–34.
15. Wnek GE, Carr ME, Simpson DG, Bowlin GL. Electrospinning of nanofiber fibrinogen structures. Nano Lett. 2003;3(2):213–6.
16. Chen M, Patra PK, Warner SB, Bhowmick S. Optimization of electrospinning process parameters for tissue engineering scaffolds. Biophys Rev Lett. 2006;1(2):153–78.
17. Yoshimoto H, Shin YM, Terai H, Vacanti JP. A biodegradable nanofiber scaffold by electrospinning and its potential for bone tissue engineering. Biomaterials. 2003;24(12):2077–82.
18. Kim K, Yu M, Zong XH, Chiu J, Fang DF, Seo YS, et al. Control of degradation rate and hydrophilicity in electrospun non-woven poly(D, L-lactide) nanofiber scaffolds for biomedical applications. Biomaterials. 2003;24(27):4977–85.
19. Yang F, Murugan R, Wang S, Ramakrishna S. Electrospinning of nano/micro scale poly(L-lactic acid) aligned fibers and their potential in neural tissue engineering. Biomaterials. 2005;26(15):2603–10.
20. Xu CY, Inai R, Kotaki M, Ramakrishna S. Aligned biodegradable nanofibrous structure: a potential scaffold for blood vessel engineering. Biomaterials. 2004;25(5):877–86.
21. Chen F, Li XQ, Mo XM, He CL, Wang HS, Ikada Y. Electrospun chitosan-P(LLA-CL) nanofibers for biomimetic extracellular matrix. J Biomater Sci Polym Ed. 2008;19(5):677–91.
22. Xu CY, Inai R, Kotaki M, Ramakrishna S. Electrospun nanofiber fabrication as synthetic extracellular matrix and its potential for vascular tissue engineering. Tissue Eng. 2004;10(7–8):1160–8.
23. Mo XM, Xu CY, Kotaki M, Ramakrishna S. Electrospun P(LLA-CL) nanofiber: a biomimetic extracellular matrix for smooth muscle cell and endothelial cell proliferation. Biomaterials. 2004;25(10):1883–90.
24. Kim TG, Park TG. Biomimicking extracellular matrix: cell adhesive RGD peptide modified electrospun poly(D, L-lactic-Co-glycolic acid) nanofiber mesh. Tissue Eng. 2006;12(2):221–33.
25. Bolgen N, Menceloglu YZ, Acatay K, Vargel I, Piskin E. In vitro and in vivo degradation of non-woven materials made of poly(epsilon-caprolactone) nanofibers prepared by electrospinning under different conditions. J Biomater Sci Polym Ed. 2005;16(12):1537–55.
26. Li WJ, Danielson KG, Alexander PG, Tuan RS. Biological response of chondrocytes cultured in three-dimensional nanofibrous poly(epsilon-caprolactone) scaffolds. J Biomed Mater Res A. 2003;67A(4):1105–14.
27. Stitzel J, Liu L, Lee SJ, Komura M, Berry J, Soker S, et al. Controlled fabrication of a biological vascular substitute. Biomaterials. 2006;27(7):1088–94.
28. Ashammakhi N, Ndreu A, Piras A, Nikkola L, Sindelar T, Ylikauppila H, et al. Biodegradable nanomats produced by electrospinning: expanding multifunctionality and potential for tissue engineering. J Nanosci Nanotechnol. 2006;6(9–10):2693–711.
29. Martins A, Reis RL, Neves NM. Electrospinning: processing technique for tissue engineering scaffolding. Int Mater Rev. 2008;53(5):257–74.
30. Barnes CP, Sell SA, Boland ED, Simpson DG, Bowlin GL. Nanofiber technology: designing the next generation of tissue engineering scaffolds. Adv Drug Deliv Rev. 2007;59(14):1413–33.
31. Pham QP, Sharma U, Mikos AG. Electrospinning of polymeric nanofibers for tissue engineering applications: a review. Tissue Eng. 2006;12(5):1197–211.
32. Vaz CM, van Tuijl S, Bouten CVC, Baaijens FPT. Design of scaffolds for blood vessel tissue engineering using a multi-layering electrospinning technique. Acta Biomater. 2005;1(5):575–82.
33. Ayres C, Bowlin GL, Henderson SC, Taylor L, Shultz J, Alexander J, et al. Modulation of anisotropy in electrospun tissue-engineering scaffolds: analysis of fiber alignment by the fast Fourier transform. Biomaterials. 2006;27(32):5524–34.
34. Baker BM, Mauck RL. The effect of nanofiber alignment on the maturation of engineered meniscus constructs. Biomaterials. 2007;28(11):1967–77.
35. Li D, Ouyang G, McCann JT, Xia YN. Collecting electrospun nanofibers with patterned electrodes. Nano Lett. 2005;5(5):913–6.
36. Li D, Wang YL, Xia YN. Electrospinning of polymeric and ceramic nanofibers as uniaxially aligned arrays. Nano Lett. 2003;3(8):1167–71.
37. Dalton PD, Klee D, Moller M. Electrospinning with dual collection rings. Polymer. 2005;46(3):611–4.
38. Zhang DM, Chang J. Patterning of electrospun fibers using electroductive templates. Adv Mater. 2007;19:3664–7.
39. Lee CH, Shin HJ, Cho IH, Kang YM, Kim IA, Park KD, et al. Nanofiber alignment and direction of mechanical strain affect the ECM production of human ACL fibroblast. Biomaterials. 2005;26(11):1261–70.
40. Li WJ, Mauck RL, Cooper JA, Yuan XN, Tuan RS. Engineering controllable anisotropy in electrospun biodegradable nanofibrous scaffolds for musculoskeletal tissue engineering. J Biomech. 2007;40:1686–93.
41. Zhang DM, Chang J. Electrospinning of three-dimensional nanofibrous tubes with controllable architectures. Nano Lett. 2008;8(10):3283–7.
42. Alexander J, Fuss B, RJ C. Electric field-induced astrocyte alignment directs neurite outgrowth. Neuron Glia Biol. 2006;2:93–103.